γ-RAY EMISSION AND PARTICLE ACCELERATION IN PLERIONS

A. K. HARDING
Code 661, NASA Goddard Space Flight Center, Greenbelt, MD 20771, USA

O. C. DE JAGER
Department of Physics, Potchefstroom University, 2520 Potchefstroom, South Africa

The luminous nebulae (plerions) surrounding many pulsars radiate radio, optical or X-ray synchrotron emission and are sites of particle acceleration. The synchrotron emitting, relativistic electrons will produce an additional component due to inverse Compton scattering that is, in some cases, detectable at gamma-ray energies. The Crab nebula is the archetypical example of a gamma-ray plerion and was the first detected TeV gamma-ray source. The observed spectrum is consistent with predictions of synchrotron-self Compton models. Inverse-Compton scattering on other soft photon sources, particularly the 2.7K microwave and galactic far-infrared backgrounds, may also be producing TeV emission in other plerions. This paper will review such models for gamma-ray emission and what the observed emission implies for particle acceleration in plerions.

1 Introduction

A number of isolated pulsars are surrounded by compact nebulae which appear to be powered by their spin-down luminosity. This kind of nebulae, called plerions (filled supernova remnants) are both energetically and morphologically distinct from conventional, shell-type supernova remnants that are driven ultimately by the binding energy release of the supernova core collapse. Two of the half-dozen sources of Very-High-Energy (TeV) γ-rays are known plerions, the Crab[44] and Vela[46] nebulae, and another unpulsed TeV source[26] is at the location of a suspected X-ray[7] and radio[14] plerion surrounding the radio and γ-ray pulsar PSR1706-44. Clearly, these sources stand out in the high-energy sky as prime particle accelerators. In contrast, the shell-type supernova remnants that have long been suspected accelerators of cosmic-ray particles have not been detected as TeV sources[29] (see review by Baring[5]).

Plerions form when the relativistic wind from a pulsar, which is thought to carry the bulk of its spin-down power[36,25] is confined by a more slowly expanding ($v_{\rm exp} \ll c$) shell of the surrounding supernova remnant. The spin-down energy of the pulsar may then be dissipated in a shock which accelerates the particles and randomizes their pitch angles. The emission at TeV energies from the Crab nebula can be explained as inverse Compton scattering of the synchrotron radiation by the relativistic particles in the plerion. Calculated synchrotron-self Compton spectra provide a very good fit to the observed γ-ray spectrum of the Crab[11,4].

Predicted synchrotron-self Compton (SSC) fluxes of the other plerions associated with pulsars would not be detectable at TeV energies. Their magnetic fields are lower than that of the Crab, and the synchrotron radiation energy density drops below that of external sources of soft photons, including the cosmic 2.7K microwave, galactic far-infrared and starlight backgrounds. The inverse Compton γ-ray emission in these plerions will then be primarily due to scattering of synchrotron-emitting electrons with external soft photon backgrounds.

The observed spectrum from hard X-rays to TeV γ-rays can give us valuable information and constraints on the particle acceleration in plerions. Identifying the location of the synchrotron cutoff can measure the maximum energy of the particles[9]. Modeling the inverse Compton component can constrain the magnetic field distribution, and thus better our understanding of how the pulsar wind transfers spin down energy to particles.

2 Inverse-Compton Scattering in Plerions

The spectrum of inverse-Compton (IC) scattered radiation is computed by

$$F(\epsilon) = \epsilon \int d\nu \int dr \int d\gamma\, U(\nu, r)\, N_e(\gamma, r) \frac{d^2 N_{\gamma,\epsilon}}{dt d\epsilon}, \tag{1}$$

where $U(\nu, r)$ is the density of soft photons, $N_e(\gamma, r)$ is the spectrum of relativistic electrons and $d^2 N_{\gamma,\epsilon}/dt d\epsilon$ is the production rate of scattered photons with energy ϵ. In principle, $N_e(\gamma, r)$ can be derived in several different ways: 1) obtain the electron spectrum by inverting the observed synchrotron spectrum, assuming a magnetic field distribution and 2) compute the electron spectrum through a kinetic equation that includes an assumed injection, radiation and adiabatic losses, as well magnetic field spatial distribution, matching to the observed synchrotron spectrum. Neither method provides a unique solution, and several assumptions are required in both cases.

In the first approach[17,18,38,11], the electron spectrum $N_e(\gamma, r)$ can be obtained through inversion of the expression,

$$4\pi d^2 F_{\rm syn}(\nu, r) = \int P(\nu, r)\, N_e(\gamma, r)\, d\gamma, \tag{2}$$

where $P(\nu, r)$ is the synchrotron emissivity, $F_{\rm syn}$ is the observed synchrotron spectrum and d is the distance to the source, assuming a nebular magnetic field distribution as a function of radius r. The kinetic equation approach has been applied to models of the Crab nebula by Stepanian[42].

2.1 Magnetic Field of a Plerion

A major source of uncertainty in computing IC fluxes is the magnetic field distribution in the plerion. The magnetic field cannot be measured directly, but there are several indirect methods of determining its average value or its distribution. If the synchrotron spectrum of the plerion shows a well-defined break in slope or power-law index at frequency, ν_B, assumed to be caused by a break in the electron spectrum at the energy where the synchrotron cooling time equals the plerion age in years, $\tau_{\rm yr}$, then the average magnetic field is

$$\langle B_\perp \rangle = 1.1\,{\rm G}\left(\frac{\nu_B}{10^9\,{\rm Hz}}\right)^{-1/3} \tau_{\rm yr}^{-2/3}. \tag{3}$$

The break at $\nu_B \approx 10^{13}$ in the spectrum of the Crab nebula[32] gives $\langle B_\perp \rangle \approx 3 \times 10^{-4}$ G.

In the absence of a measured break in the plerion spectrum, an estimate of the equipartition field can be obtained by balancing the energy density of the magnetic field, $B_{\rm eq}^2/8\pi$ with an inferred particle density. Assuming equipartition of field and particle density in the pulsar wind[36],

$$\frac{B_{\rm eq}^2}{8\pi} = \frac{1}{2}\frac{L}{4\pi r_s^2 c}. \tag{4}$$

where, L is the spin-down luminosity of the pulsar and $r_s = v_{\rm exp}\,\tau\sqrt{\frac{v_{\rm exp}}{3c}}$ is the radius of the pulsar wind termination shock. This gives a value,

$$B_{\rm eq} = 3 \times 10^{-4}\,{\rm G}\; B_{12}\, P^{-2}\, \tau_{\rm yr}^{-1}\, v_8^{-3/2} \tag{5}$$

where $B_{12} \equiv B_o/10^{12}$ G is the pulsar surface field strength, P is the pulsar period and $v_8 \equiv v_{\rm exp}/10^8\,{\rm cm\,s^{-1}}$ is the expansion velocity of the plerion. For the Crab nebula, with $v_{\rm exp} = 1500\,{\rm km\,s^{-1}}$, $B_{\rm eq} \simeq 4 \times 10^{-4}$ G, in good agreement with the magnetic field value determined from the spectral break. Another estimate for the equipartition field can be found by balancing the magnetic energy with the inferred energy of the synchrotron emitting particles[8]. If the observed synchrotron spectrum is $S(\epsilon_{keV}) = S_{1keV}\,\epsilon_{keV}^{-a_x}$, where S_{1keV} is the X-ray flux at 1 KeV and α_x is the energy index, then

$$B_{\rm eq} = 1.1 \times 10^{-4}\,{\rm G}\left[\frac{\kappa\, S_{1keV}}{(\theta\, d_{kpc})^3\,\alpha(p)\,(2a_x - 1)}\right]^{2/7} \tag{6}$$

where θ is the angular radius of the plerion in arcmin, and d_{kpc} is the source distance in kpc. The function $\alpha(p)$ of the electron spectral index $p = 2a_x + 1$ comes from the synchrotron inversion formula[28], and the factor $\kappa = [\epsilon_{kev}^{min}]^{(1-2a_x)/2} - [\epsilon_{kev}^{max}]^{(1-2a_x)/2}$, comes from integrating over the range ϵ_{kev}^{min} to ϵ_{kev}^{max} over which the power law spectrum is valid.

2.2 Soft Photon Density

For each plerion, $U(\nu, r)$ will include several different soft photon sources: (1) synchrotron radiation of the plerion (2) 2.7K microwave background radiation (3) local infrared radiation from dust (4) galactic infrared background radiation and 5) galactic starlight. Generally, only the youngest plerions, having the strongest nebular magnetic fields, will have a dominant synchrotron-self Compton contribution. In the older plerions, the inverse Compton emission will be due primarily to scattering of the relativistic electrons with sources of background photons. The relative

Table 1: Predicted and Detected Inverse Compton Flux From X-Ray Plerions

Source	B_{eq} (μG)	S_{1keV} (cm^{-2} s^{-1})	a_x	S_{MBR}(1TeV) (cm^{-2} s^{-1})	S_{FIR}(1TeV) (cm^{-2} s^{-1})	S_{det}(1TeV) (cm^{-2} s^{-1})
Crab	223	10	1.15	1.6 (-12)	1.5 (-12)	2.0 (-11)[44]
Vela (compact)	95	.01	0.73	8.0 (-15)	3.3 (-15)	
Vela (TeV source)	2.6	.0012	1.1	2.2 (-12)	2.5 (-12)	6.0 (-12)[46]
PSR1706-44	3.0	.0005	1.4	2.0 (-12)	7.5 (-12)	8.0 (-12)[26]
MSH15-52	6.0	.027	0.6	1.7 (-12)	7.5 (-13)	<8.3 (-12)[13]
CTB80 (PSR1951+32)	1.8	.0003	1.1	1.2 (-12)	1.4 (-12)	<5.4 (-12)[27]
PSR0656+14						<3.4 (-11)[37]
PSR1055-52						<1.0 (-12)[27]
Geminga						<8.9 (-12)[2]

contributions of the three main background components will depend on the plerion's proximity to the galactic plane and to the galactic center. The cosmic MBR is of course constant with location, but the far-infrared (FIR) and starlight contributions vary strongly with position in the galaxy. Various determinations of the galactic interstellar radiation field density differ significantly: for example the local FIR density derived by Strong & Youssefi[43] is 2-3 times that derived by Skibo[41]. Thus, the uncertainty in determination of the galactic photon densities is another major source of uncertainty in the computed IC fluxes from plerions.

The X-ray emitting electrons in the plerion scatter MBR and FIR photons to TeV energies. De Jager et al.[8] have obtained an expression for the TeV γ-ray flux from inverse Compton scattering of 2.7K MBR only,

$$S_{MBR}(\epsilon_{TeV}) = 6.6\times10^{-17}\, f_{KN}\, (1.4\times10^{-5})^{a_x}\, \exp(2.2a_x - 0.126a_x^2)\, B_\perp^{-(a_x+1)}\, S_{1keV}\, \epsilon_{TeV}^{-a_x}\, \mathrm{s}^{-1}\,\mathrm{cm}^{-2}, \quad (7)$$

assuming an observed X-ray synchrotron spectrum of the form given in Sec. 2.1. The factor $f_{KN} = [1 - H(a_x)\sqrt{\epsilon_{TeV}\, kT}/mc^2]$ is a first order correction to the Thomson limit of the Compton scattering cross section, and approximates the spectral steepening due to the declining Klein-Nishina cross section. An expression for $H(a_x)$ in the range $0 \le a_x \le 2.5$ is given by $H(a_x) = 2.4 + 3.9\, a_x + 0.42\, a_x^2$. Note, in the Thomson limit, that the index of the TeV spectrum is predicted to be the same as that of the X-ray spectrum. Since the far-infrared photon density is comparable to or greater than the MBR density in most of the galaxy, the formula given in Eqn (7) will underestimate the total IC flux. Thus, one should add the contribution due to scattering on the FIR (25K) background radiation density, U_{25}, given by

$$S_{FIR}(\epsilon_{TeV}) = 0.023\, (25/2.7)^{a_x}\, (a_x + 4)(a_x + 3)\, U_{25}\, S_{MBR}(\epsilon_{TeV}) \quad (8)$$

where U_{25} is in units of eV/cm^3.

Table 1 shows the computed values of IC flux for a number of plerions using Eqns (6),(7) and (8) as well as detected fluxes and upper limits from different telescopes. The total predicted flux would be the sum of $S_{\mathrm{MBR}}(1TeV)$ and $S_{\mathrm{FIR}}(1TeV)$ and may be less than the actual flux because scattering from starlight, local dust components and SSC emission has not been included.

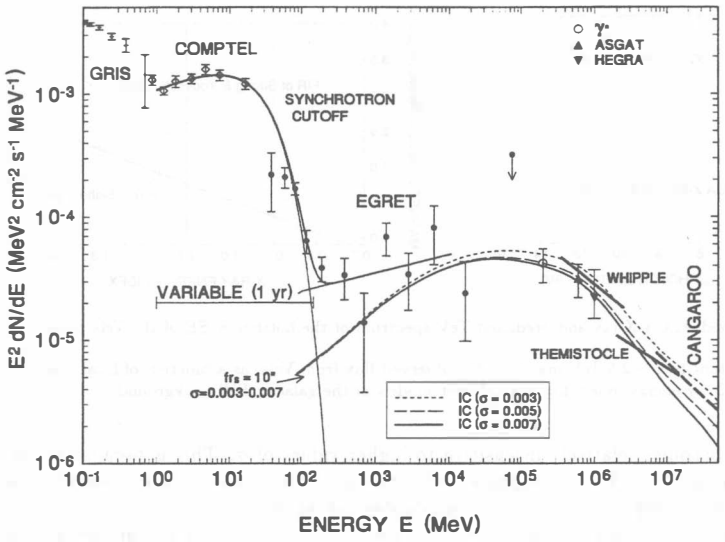

Figure 1: Observed and model gamma-ray spectra of the Crab nebula. Data is from GRIS[6], COMPTEL[33], EGRET[9], γ^{*1}, Whipple[45], ASGAT[16], Themistocle[12], HEGRA[35] and Cangaroo[15].

3 Emission from Detected Gamma-Ray Plerions

3.1 Crab Nebula

The Crab nebula is the only plerion with a presently detectable SSC flux. In fact, from the estimate in Table 1, scattering of external photon backgrounds contributes only $\sim 10\%$ of the observed flux. LMC0540-69 has a larger value of $B_{\rm eq}$ but is 25 times more distant. Vela X, with a field 15 times smaller, has a predicted SSC flux about a tenth that of the Crab. The SSC model for the Crab began its development over 30 years ago, before any TeV observations had been made, when Gould[17] predicted there might be a detectable flux. The early models assumed a constant field strength in the nebula[17,38] or a simple assumed radial field dependence[18]. Now that many different air-Cherenkov telescopes have detected the Crab and we have an accurate measurement of the spectrum in the 0.2 - 10 TeV range, the SSC models have evolved in sophistication. De Jager & Harding[11] (DH) used the magnetic field distribution derived from the MHD flow model of Kennel & Coroniti[25] (KC) to invert the observed synchrotron spectrum. The MHD flow solutions of KC are described by a parameter, σ, the ratio of magnetic energy to particle energy in the wind at the termination shock (at r_s). KC found that the solution which best matched the boundary condition ($v_{\rm exp} = 1500\,{\rm km\,s^{-1}}$) at the outer edge of the nebula required that σ be very small ($\approx .003$), so that the wind is particle dominated. The magnetic field distribution for this solution increases with r downstream of the shock as $B(r) \propto r$ until equipartition is reached, after which it decreases as $B(r) \propto 1/r$. The magnetic field at the shock is much smaller than equipartition value for small σ but for large values of $\sigma > 1$, the field approaches equipartition everywhere and $B(r) \propto 1/r$. DH found that the SSC spectrum and flux using the KC best fit solution agrees with the measured spectrum at TeV energies. Figure 1 shows the current measurements of the Crab nebula γ-ray spectrum and the SSC model fits from De Jager et al.[9]. The measurements in the TeV range give a good lower limit, $\sigma \gtrsim .003$,

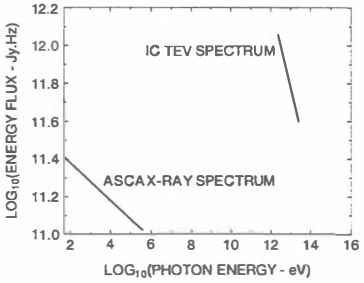

Figure 2: The observed ASCA X-ray and predicted TeV spectrum of the hotspot 8' SE of the Vela pulsar.

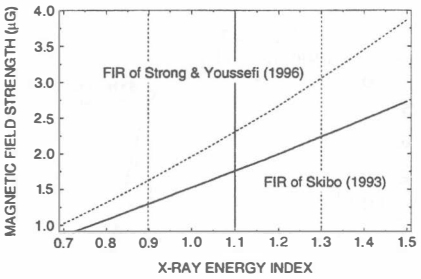

Figure 3: Lines of constant flux > 2.5 TeV matching the observed flux from Vela, as a function of local magnetic field and X-ray energy index, for two different models of the galactic FIR background.

but the model flux becomes relatively insensitive to higher values of σ. This is because the IC emission at TeV energies and below originates from the entire nebula and thus measures the average magnetic field strength, which is only weakly dependent on σ.

With a good model for the Crab TeV flux and spectrum, and thus for the magnetic field strength in all parts of the nebula, one can predict the maximum energy of particles accelerated by the first-order Fermi mechanism (see Baring[5] and Sec. 5) at the pulsar wind shock. De Jager et al.[9] found that this energy was about 5×10^{15} eV, which gives a synchrotron cutoff at ~ 25 MeV, about where a cutoff is observed by the EGRET and COMPTEL instruments on CGRO.

The KC model applies to the MHD flow in the pulsar spin equatorial plane and is intrinsically 1-D. There is, in fact, a torus-like shape seen in the nebular X-ray emission[3], indicating that the equatorial wind is probably the site of the high energy synchrotron emission. However, the radio and optical emission shows more of an hourglass shape, oriented perpendicular to the X-ray torus, whose long axis is now thought to be aligned with the pulsar spin axis[22]. This 3-D nature of the Crab pulsar wind and nebula should be taken into account in the next-generation SSC models.

3.2 Vela

The CANGAROO telescope has recently reported unpulsed emission above 2.5 TeV from the Vela region[46]. The peak of this emission is not centered on the 1' compact nebula surrounding the pulsar, seen at optical and X-ray wavelengths, but is located 8' southeast of the pulsar. The ROSAT PSPC map of the region[31] shows a spot of emission at the location of the TeV source, which is also the inferred birth location of the pulsar, based on its age and measured proper motion. The magnetic field of the compact nebula is estimated to be[8,10] $\sim 60\,\mu$G, which gives a predicted IC flux too small to be detectable (see Table 1).

The spectrum of the X-ray hotspot at the Vela birthplace has been obtained from ASCA archival data in the 1 - 10 keV band[21] and is consistent with a power law with parameters given in Table 1. Assuming that this X-ray emission is synchrotron radiation, Eqn (6) gives a magnetic field around 2 μG, much lower than the field of the compact nebula. The predicted IC emission from scattering on the MBR and FIR backgrounds is thus much higher and can account for the observed flux (see Table 1). Figure 2 shows the observed X-ray spectrum and computed IC spectrum, assuming a field of 2.7 μG, using a numerical code which is more accurate than the approximate formula of Eqn (7) because it includes the full Klein-Nishina cross section and the starlight as well as MBR and FIR backgrounds. Note that the IC spectrum above 2.5 TeV is

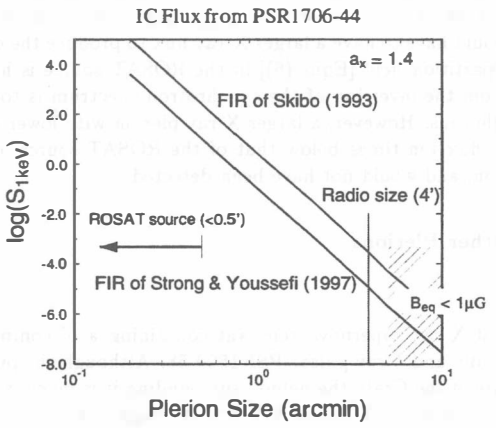

Figure 4: Lines of constant flux at 1 TeV that matches the observed flux from PSR1706-44, as a function of local magnetic field and plerion size, for two different models of the galactic FIR background.

not a single power law, but has significant curvature due to the decline of the scattering cross section. Figure 3 shows lines of constant IC flux > 2.5 TeV which matches the observed flux as a function of X-ray energy index and magnetic field for the derived values of FIR photon density of Skibo[41] and Strong & Youssefi[43]. The vertical lines mark the range of uncertainty in the measured X-ray spectral index. Given the combined uncertainties in the X-ray spectrum and the FIR photon density, the acceptable magnetic field strength in the hotspot lies between 1.3 and 3 μG.

Thus, the reported VHE emission from Vela may be due to the scattering of long-lived electrons left in a trail by the pulsar as it moved away from its birthplace. The synchrotron lifetime of these particles from $\tau = 10^5$ yr $B_\perp^{-3/2}(\mu G)\,\epsilon_{keV}^{-1/2}$, taking the derived range of $B_\perp$ from Fig. 2, is in the range $\tau \simeq 2 - 7 \times 10^4$ yr, several times the age of the pulsar. This assumes that the particles have lived in a low magnetic field environment since they were accelerated to their present energies, which would imply that the pulsar initially moved at a much higher space velocity or had a much lower field than presently observed. This latter possibility has been suggested by Muslimov & Page[34] to explain the anomalously low measured braking index of the pulsar[30].

3.3 PSR1706-44

Unpulsed emission above 2.5 TeV from the position of the radio and γ-ray pulsar PSR1706-44 was reported by the CANGAROO collaboration[26]. The lack of a pulsed signal argues in favor of plerion emission, possibly IC scattering of background radiation as for Vela, but in this case the peak of emission is centered on the pulsar. A 4' compact radio nebula surrounding PSR1706-44 has been detected by Frail et al.[14], and a point-like (< 0.5') X-ray source at the pulsar position has been detected by ROSAT[7]. The ROSAT source is less than 18% pulsed at the pulsar period and can be fit with a power law spectrum (energy index 1.4); thus a synchrotron nebula is the favored interpretation.

Figure 4 shows lines of constant IC flux > 1 TeV which matches the observed flux, computed using Eqns (6),(7) and (8), as a function of size and X-ray flux of a plerion for the derived values of FIR photon density of Skibo[41] and Strong & Youssefi[43]. The observed flux and size limit for the ROSAT source is shown and lies well below both curves, indicating that IC emission from electrons in a region of size < 0.5' would have to have a larger X-ray flux to produce the observed emission. That is because the equipartition field [Eqns (6)] in the ROSAT source is high, and thus the derived electron density from the inversion of the synchrotron spectrum is too low to scatter enough of the background photons. However, a larger X-ray plerion with lower flux, say the size of the radio plerion with a flux ten times below that of the ROSAT source, could be producing the observed TeV emission, and would not have been detected.

4 Predicted Emission from Other Plerions

4.1 MSH15-52 (PSR1509-58)

MSH15-52 is an extended radio and X-ray supernova remnant containing a 6' compact synchrotron nebula[40], centered on the radio and γ-ray pulsar PSR1509-58. Although the pulsar has an age $\sim 10^3$ yr, very close to the age of the Crab, the nebula surrounding it is much larger and the equipartition magnetic field is therefore much lower. The ASCA image of this source in the 1 - 10 KeV band shows the compact nebula, a thermal source about 7' to the N and evidence for a bridge or a jet between the two sources. Du Plessis et al.[13] have computed the IC flux from the compact source in MSH15-52, inverting the observed radio and X-ray synchrotron spectrum assuming various magnetic fields. They find that scattering on MBR dominates and the flux at TeV energies should be detectable for field strengths $B < 7\mu$G.

4.2 X-Ray Plerions

CTB80 is another detected X-ray plerion listed in Table 1, with its derived value of B_{eq} from [Eqns (6)] and predicted IC flux from scattering on MBR and FIR backgrounds from Eqns (7) and (8). CTB80 is a supernova remnant containing a compact plerion surrounding PSR1951+32, a radio and γ-ray pulsar, has an X-ray spectrum measured by ROSAT[89] and is also a radio source[15]. The predicted emission at 1 TeV is close to the sensitivity level of current telescopes. ASCA has detected extended emission around a number of pulsars which could be synchrotron nebulae[24], including PSR0656+14, PSR1055-52, Geminga and PSR1929+10. However, since the spectra of these extended X-ray components are not yet available, TeV flux predictions for these sources have not been included in Table 1. Several of these sources have published TeV flux upper limits which are listed in the Table.

5 Particle Acceleration in Plerions

The presence of relativistic particles in X-ray synchrotron nebulae whose sizes are many light crossing times larger than the radiation loss times of the particles requires *in situ* acceleration. That is, the synchrotron emitting particles cannot have been accelerated in the pulsar magnetosphere and retained their energy against losses near the pulsar or in the nebula. The most likely *in situ* acceleration site is the termination shock of the pulsar wind. The shock radius, discussed in 2.1, is at a large distance from the pulsar, at approximately one tenth of the nebula radius in the Crab. The wind which flows out along the open field lines of the pulsar magnetosphere (i.e. those which cross the speed of light cylinder at a distance $R_{LC} = c/\Omega$ from the pulsar) carries a potential drop equal to

$$V \approx 6.5 \times 10^{12}\,\mathrm{eV}\, P^{-2}\, B_{12}. \qquad (9)$$

For the Crab, $V \approx 3 \times 10^{16}$ eV, more than sufficient to supply the energy of the γ-ray emitting electrons in the nebula. The energy of this potential drop may be partially converted to particle energy at the shock through several mechanisms. Measurement of a cutoff at 25 MeV in the synchrotron spectrum of the Crab gives a maximum particle energy of $\sim 5 \times 10^{15}$ eV (DH) and detection of γ-rays up to at least 400 keV from the Vela compact nebula[10] gives a maximum energy $\gtrsim 3 \times 10^{14}$ eV. In both cases, the particle maximum energy is about 10% of the total wind potential drop, indicating that acceleration is operating very efficiently.

Harding & Gaisser[19] and DH have proposed that particles can be accelerated at the pulsar wind shock through the first-order Fermi mechanism, gaining energy by scattering back and forth across the shock front from magnetic irregularities which move with the fluid and act as converging walls (see Baring[5] for a more detailed discussion). They showed that the maximum energy gain by this process is equal to the potential drop given in Eqn (9). However, the shock in the pulsar wind is a perpendicular shock (the magnetic field is perpendicular to the shock normal) so that cross-field tranport must be present for Fermi acceleration to operate effectively. Such cross-field transport may be possible in the equatorial wind zone due to the rapid field reversals in the pulsar wind (at the frequency of the pulsar)[20]. Hoshino et al.[23], performing particle-in-cell simulations of the pulsar wind termination shock, find that in the absence of cross-field transport, positrons may be accelerated via ion magnetosonic waves.

Acceleration at the termination shock may work for the equatorial wind zone (i.e. the X-ray torus in the Crab) but acceleration in the polar wind zone is occurring as well, as evidenced by the jets observed in the Crab, Vela and possibly PSR1509-58, and has not been studied extensively.

6 Summary

The three plerion sources so far detected in very-high energy (TeV) γ-rays show a surprising variety of emission characteristics, and each tells us a different story about the origin of relativistic electrons in plerions. The TeV emission from the Crab nebula is located at the position of the well-studied radio, optical and X-ray synchrotron nebula and a synchrotron-self Compton model agrees well with the observed TeV flux and spectrum. The inferred characteristics of the relativistic electron spectrum is consistent with acceleration in the pulsar wind termination shock. The TeV emission from the two older ($\tau \sim 10^4$ yr) sources might be explained as inverse Compton scattering on the MBR and other soft photon backgrounds rather than as SSC and is more complicated. Although a TeV emission peak is located at the position of PSR1706-44 and its radio nebula, the relativistic electrons needed to account for the X-ray flux at this position cannot produce the observed TeV flux unless there is an undetected fainter, more extended X-ray nebula. The TeV emission in Vela is apparently not coming from the compact nebula, but from an X-ray hotspot at the purported birthplace of the pulsar. If the pulsar left relativistic electrons behind it as it moved to its present position, then their very long lifetimes suggest that the pulsar magnetic field must have been much lower shortly after its birth. If the γ-ray emission is mapping out the location of the most energetic particles, it is telling us that the pulsar spin-down energy which goes into these particles becomes less centralized around the pulsar as it ages, and is accompanied by stronger jets and more extended emission. As we discover more plerions in high-energy γ-rays, we may begin to understand the evolution of the energy budget of a pulsar and its environs.

References

1. C.W. Akerlof *et al.* in *Proc. GRO Workshop* (GSFC), 4-49.
2. C.W. Akerlof *et al.* A & A **274**, L17 (1993).

3. B. Aschenbach & W. Brinkmann, A & A **41**, 147 (1975).
4. A.M. Atoyan & F.A. Aharonian MNRAS **278**, 525 (1996).
5. M.G. Baring, these proceedings.
6. L.M. Bartlett, Ph.D. Thesis, Univ. of Maryland (1994).
7. W. Becker, K.T.S. Brazier & J. Trumper A & A **298**, 528 (1995).
8. O. C. De Jager, A. K. Harding, M. G. Baring & A. Mastichiadis, *in Proc. 24rd Int. Cosmic Ray Conf.*(1995).
9. O.C. De Jager *et al.* ApJ **457**, 253 (1996).
10. O.C. De Jager, A.K. Harding & M.S. Strickman ApJ **460**, 729 (1996).
11. O.C. De Jager & A.K. Harding ApJ **396**, 161 (1992).
12. A. Djannati-Atai, Ph.D. Thesis, Univ. of P. et M. Curie (Paris), (1994).
13. I. Du Plessis *et al.* ApJ **453**, 746 (1995).
14. D.A. Frail, W.N. Goss & J.B.Z. Whiteoak ApJ **437**, 781 (1994).
15. A.S. Fruchter *et al.* Nature **331**, 53 (1988).
16. P. P. *et al.* A & A **270**, 401 (1993).
17. R.J. Gould Phys. Rev. Lett. **15**, 577 (1965).
18. J.E. Grindlay & J.A. Hoffman Astrophys. Lett **8**, 209 (1971).
19. A.K. Harding & T.K. Gaisser ApJ **358**, 561 (1990).
20. A. K. Harding, F. C. Jones & O. C. De Jager, in *23rd Int. Cosmic Ray Conf.***1**,279 (1993).
21. A. K. Harding, O. C. De Jager & E. Gotthelf, in *25th Int. Cosmic Ray Conf.*,in press, (1997).
22. J. J. Hester *et al.* ApJ **448**, 240 (1995).
23. M. Hoshino *et al.* ApJ **390**, 454 (1992).
24. N. Kawai & K. Tamura, in *Pulsars: Problems and Progress, IAU Coll. 160*, in press, 1997.
25. C.F. Kennel & F.V. Coroniti, F.V. ApJ **283**, 694 (1984).
26. T. Kifune *et al.* ApJ **438**, L91 (1995).
27. T. Kifune in *Pulsars: Problems and Progress, IAU Coll. 160*, in press, 1997.
28. K.R. Lang, *Astrophysical Formulae*(Springer-Verlag,New York, 1974), p. 35.
29. R.W. Lessard *et al.*, in *24th Int. Cosmic Ray Conf.***2**, 425 (1995).
30. A.G. Lyne, R. N. Manchester & N. Amico Nature **460**, 41 (1996).
31. C.B. Markwardt & H. Ogelman Nature **375**, 40 (1995).
32. P.L. Marsden *et al.* A & A **278**, L29 (1984).
33. R.P. Much *et al.* Adv. Space Res. **15(5)**, 81 (1995).
34. A. Muslimov & D. Page, in *Proc. Acad. Coll. on Pulsar Timing, General Relativity and the Internal Structure of Neutron Stars*, (Kluwer, Amsterdam) (1997).
35. D. Petry *et al.* A & A **311**, 13 (1996).
36. M.J. Rees & J.E.Gunn ApJ **167**, 1 (1974).
37. P.T. Reynolds *et al.*, ApJ **404**, 206 (1993).
38. G.H. Rieke & T.C. Weekes ApJ **155**, 429 (1969).
39. A. Safi-Harb, H. Ogelman & J.P. Finley, ApJ **439**, 722 (1995).
40. F.D. Seward *et al.* ApJ **267**, 698 (1983).
41. J. Skibo, Ph.D. Thesis, Univ. Maryland, (1993).
42. A.A. Stepanian, in *Proc. Vulcano Workshop 1990*, (IPS, Bologna,Italy), p.377 (1990).
43. A.W. Strong & G. Youssefi, *A & A*, submitted, (1997).
44. T.C. Weekes et al., ApJ **342**, 379 (1989).
45. T.C. Weekes, paper presented at Veritas Workshop (1997).
46. T. Yoshikoshi, Ph.D. Thesis, Univ. of Tokyo, (1996).